Energy loss of nuclear fragments in partially ionized materials of high atomic number

R. A. Lewis, G. A. Smith, and W. S. Toothacker
Laboratory for Elementary Particle Science, Department of Physics, Pennsylvania State University, University Park, Pennsylvania 16802
(Received 1 November 1990; revised manuscript received 15 February 1991)

Methods used for the computation of the stopping power of high-atomic-number media to light and heavy nuclear fragments in un-ionized and completely ionized states are reasonably well developed. This is not the case for partially ionized states. We propose a method that bridges these two extremes and discuss applications of the method to α particles and fission fragments in uranium at extreme temperatures and densities.

I. INTRODUCTION

To predict effects of nuclear-particle interactions in targets, models of energy deposition over a wide range of temperature and density are required. We are interested in understanding the energy profile due to low-energy antiprotons that come to rest in uranium and induce fission. This process has recently been observed at the Low Energy Antiproton Ring (LEAR) at CERN [1–3]. Because this fission occurs with nearly 100% probability and emits ~180 MeV of locally deposited fission fragment energy, it may be an efficient way of producing conditions of high pressure, temperature, and compression in a target of fissile material. This possibility was first pointed out by Polikanov in 1982 [4]. This leads to questions concerning the stopping power of cold and hot uranium to fission fragments, as well as light nuclear fragments such as α particles resulting from fusion within a target partially filled with isotopes of hydrogen.

The theory of the stopping power of ions in cold material is well developed, and is readily tested and accessible in the program TRIM85 [5]. The theory for a completely ionized material is also understood and described in the literature [6]. However, the stopping power of a partially ionized, high-atomic-number medium is not well described, in part due to lack of experimental data at the extreme temperatures of interest.

We first briefly review stopping-power theory in cold materials (Sec. II). This is followed by a detailed description of a generalized approach to describing stopping power in partially ionized media (Sec. III), an application to α particles and fission fragments in uranium (Sec. IV), and finally conclusions (Sec. V).

II. STOPPING POWER IN COLD MATERIAL

We have computed the stopping power of ions in a cold material using the program TRIM85. Figure 1 shows dE/dx versus energy for typical fission fragments (^{119}Sn ions) in cold uranium. The electronic stopping power rises to a maximum, and then decreases monotonically with increasing ion energy. The region above the maximum is described by Bohr theory [7,8]. In this region, the ion velocity (v) is larger than the velocity of electrons in the uranium. The time of collision between the ion and electron is determined by the ion velocity, leading to an approximate $1/v^2$ dependence of the stopping power.

The maximum stopping power of an α particle occurs at a specific energy of 0.2 MeV/amu [5], much lower than the peak of 5 MeV/amu for a ^{119}Sn ion. For an α particle, the maximum dE/dx occurs near the energy at which its velocity is close to the mean electron velocity in uranium. At lower velocities the collision time is governed by electron motion, resulting in a stopping power that decreases with decreasing ion velocity. For ^{119}Sn, inner-shell electrons on the projectile remain bound for velocities below the velocities of electrons bound to the uranium. The electrons on the ion provide a shield, which limits the energy transfer to electrons in the uranium. The maximum stopping power occurs at an energy for which the ^{119}Sn ion is nearly 100% stripped of its electrons.

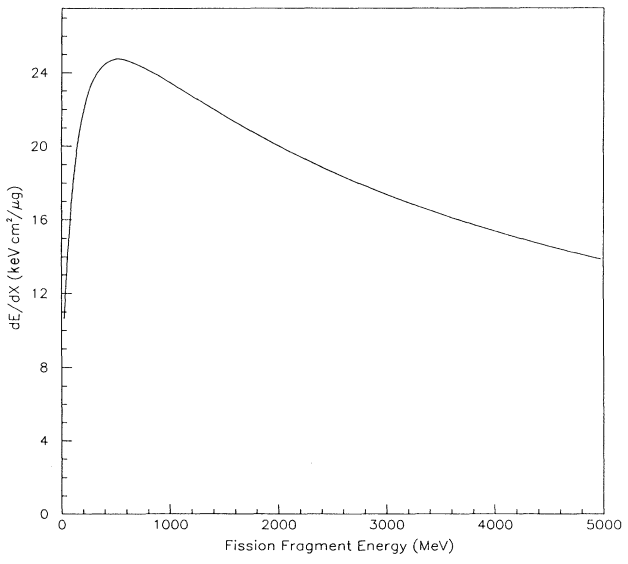

FIG. 1. Electronic energy loss of ^{119}Sn ions for energies up to 5000 MeV in cold uranium as calculated by TRIM85.

At very low velocities, far below the dE/dx maximum, the stopping power is proportional to velocity, the so-called "velocity-proportional" region. In this region, electron exchange is the mechanism for transferring energy from the ion to the uranium [9]. The contribution of nuclear scattering is calculated using the screened potentials in TRIM85 for low temperatures (<100 eV), and unscreened Rutherford scattering for higher temperatures.

III. ENERGY LOSS IN PARTIALLY IONIZED MATERIAL

One approach to describing energy loss of ions in a partially ionized medium is based on the dielectric properties of the medium [10–13]. The effects of both free and bound electrons in the medium are expressed in terms of a complex index of refraction. The moving ions excite various modes of oscillation in the plasma, leading to transfer of energy. However, the energy loss is well defined only if the ion is moving much faster than electrons in the medium.

An alternate approach that can be used for both fast and slow ion velocities is based on a separation of the effects of bound and free electrons [14], where one writes

$$\frac{dE}{dx}=\left[\frac{dE}{dx}\right]_{\text{bound}}+\left[\frac{dE}{dx}\right]_{\text{free}}+\left[\frac{dE}{dx}\right]_{\text{nuclear}} . \quad (1)$$

The state of ionization of the medium is determined from the Saha equation [15,16]. The ionization state of the ion is defined by equating the velocity of the highest bound electron in the ion to the mean relative velocity of the ion and free electrons in the medium [14,17–19].

The contribution to the stopping power by free electrons is well defined [14]. The behavior of stopping power in a free-electron plasma is similar to that in cold materials, provided one replaces the electron binding energy with the free-electron energy. The stopping power due to free electrons can be written in the form

$$\left[\frac{dE}{dx}\right]_{\text{free}}=N_e Z^2 G(y)/v^2 , \quad (2)$$

where N_e is free-electron density, Z is the net charge on the ion, and $y=v/v_{\text{electron}}$. The function $G(y)$, which depends only on the ratio of ion and electron velocities, interpolates smoothly between slow and fast ion velocities and is written in the form

$$G(y)=A[\text{erf}(y)-2\sqrt{y/\pi}e^{-y}]\ln(B\sqrt{y}) , \quad (3)$$

where A and B are constants.

For the stopping power of bound electrons, we propose a form similar to Eq. (2) above, namely

$$\left[\frac{dE}{dx}\right]_{\text{bound}}=N_b Z^2 F(y)/v^2 , \quad (4)$$

where $F(y)$ is written in the form

$$F(y)=ay^b\ln\left[\frac{c}{y}+dy\right] \quad (y>0.3) , \quad (5)$$

where a, b, c, and d are constants and N_b is the density of bound electrons in the medium. The function $F(y)$ depends only on the ratio of ion and electron velocities. Using the virial theorem, the mean bound-electron velocity is calculated from the average ionization potential of the medium, which is [14]

$$\bar{I}(Z_m)=Z_m^2/(Z_m-\bar{Z}_m)^2 I(Z_m-\bar{Z}_m) , \quad (6)$$

or [20]

$$\bar{I}(Z_m)=33Z_m(Z_m/\bar{Z}_m)^{0.85}-23Z_m , \quad (7)$$

where Z_m is the atomic number of the medium, $\bar{Z}_m$ is the net charge of atoms in the medium, and $I(Z_m-\bar{Z}_m)$ is the mean ionization potential for a cold medium with atomic number $\bar{Z}_m-\bar{Z}_m$. Equation (7) is derived from the Thomas-Fermi model of ions, in which the radius of the ion is smaller than the spacing between ions. The model thus does not apply to densities much larger than solid densities.

Equations (6) and (7) interpolate smoothly between the two extreme cases of an un-ionized medium and hydrogenlike atoms with one remaining electron, and result in mean electron velocities that are systematically lower by up to 30% than velocities calculated from a more detailed atomic theory [21].

The advantage of Eq. (4) is that the function $F(y)$ can be evaluated conveniently using the well-developed theory [5] of stopping power in a cold medium. This approach of using the ratio of ion and electron velocities as a scaling variable has been applied to cases where the ion velocity is faster than [14], or comparable to [8], the mean bound-electron velocity. We propose that Eq. (4) is generally applicable to all ion velocities. At 10 keV temperature, nuclear scattering reduces the range of 3.5-MeV α particles by $<1\%$, and 90-MeV fission fragments by $\sim 10\%$. For cold uranium, replacing the screened nuclear scattering in TRIM85 with Rutherford scattering has no appreciable effect ($<1\%$) on the ranges.

IV. APPLICATION OF GENERALIZED STOPPING-POWER FORMULATION

The concepts described above are applied to uranium to illustrate how energy deposition varies with properties of the medium. The ionization state of the uranium varies with temperature and density. The uranium is more readily ionized at low density because of the large volume of phase space for free electrons in a sparse medium. The uranium is in a state of partial ionization for temperatures up to 10 KeV, which is of interest for fusion applications. Uranium at a density of $10\rho_0$, where ρ_0 is the density at standard temperature and pressure, is about 1% ionized even when cold, due to " pressure ionization" [22,23]. At higher densities, pressure ionization must be taken into account.

Figure 2 shows how the mean bound-electron energy varies with temperature. The solid (dashed) curves were calculated using Eqs. (6) and (7), respectively. For low-density ($0.01\rho_0$) uranium, the bound-electron energy reaches a maximum of (13.6 eV) $(92^2)=115$ KeV, corre-

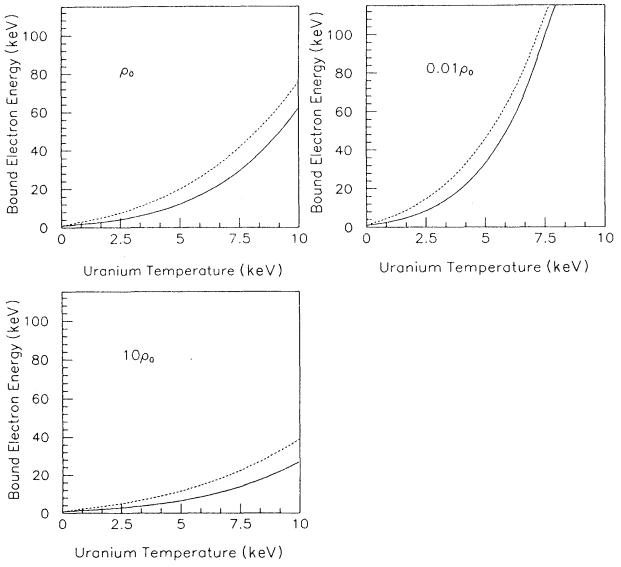

FIG. 2. Mean bound-electron energy as a function of temperature for three different uranium densities. The solid (dashed) lines were calculated using Eqs. (6) and (7), respectively.

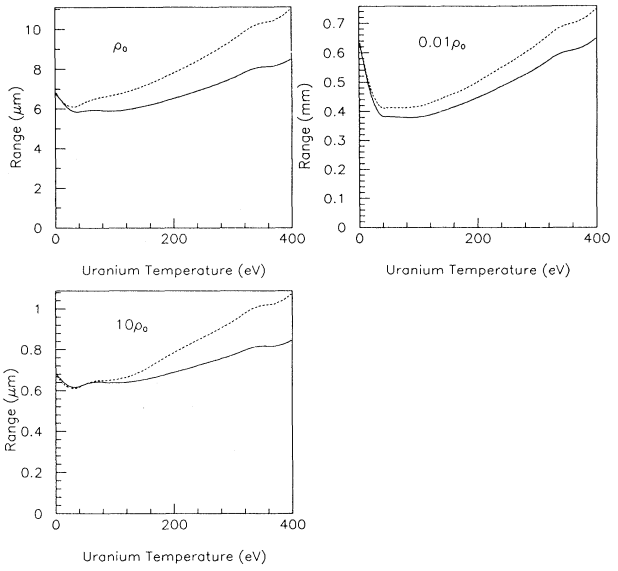

FIG. 4. Range of 3.5-MeV α particles in uranium as a function of temperature up to 400 eV for three different uranium densities. The solid (dashed) curves were calculated using Eqs. (6) and (7), respectively.

sponding to one bound electron. At temperatures above 8 KeV, the uranium is essentially 100% ionized, and the factor N_b in Eq. (4) goes to zero.

Figure 3 shows the range of a 3.5-MeV α particle in uranium at various densities as a function of temperature. The solid (dashed) curves were calculated using Eqs. (6) and (7), respectively. The "range-shortening" phenomenon often quoted in the literature [10–13] can be clearly seen by expanding the region below 400-eV temperature, as shown in Fig. 4. Compared to room temperature, the range decreases by as much as a factor of 2 for a density of $0.01\rho_0$ at temperatures around 100 eV. The

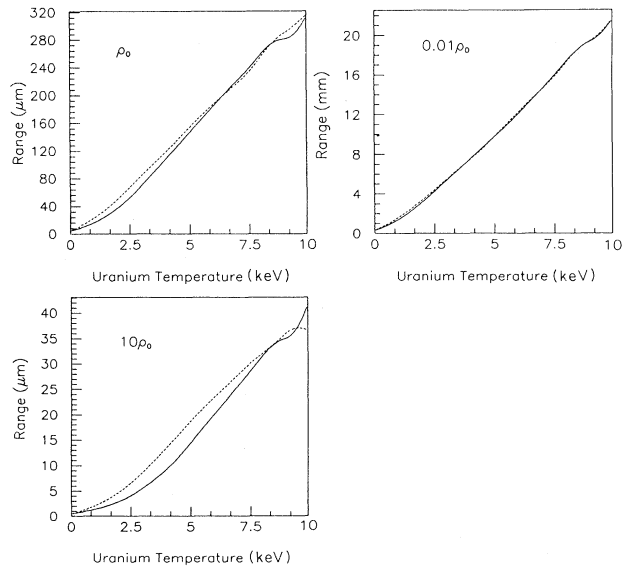

FIG. 3. Range of 3.5-MeV α particles in uranium as a function of temperature up to 10 KeV for three different uranium densities. The solid (dashed) curves were calculated using Eqs. (6) and (7), respectively.

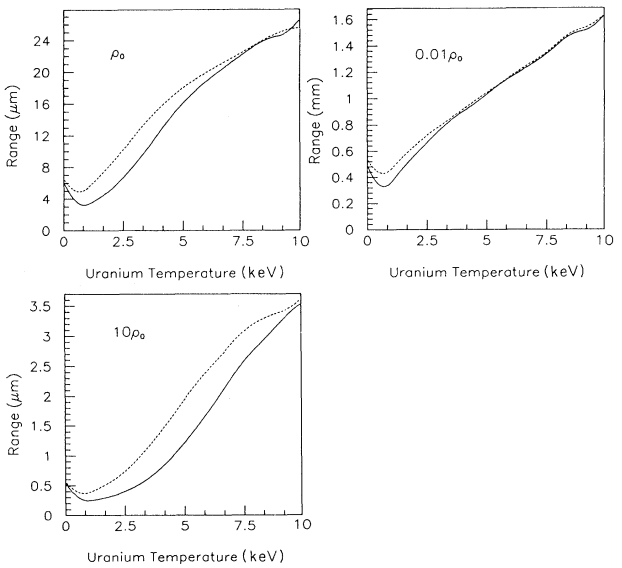

FIG. 5. Range of 90-MeV fission fragments in uranium as a function of temperature up to 10 KeV for three different uranium densities. The solid (dashed) curves were calculated using Eqs. (6) and (7), respectively.

range is decreased due to the fact that the plasma frequency of free electrons is lower than the orbital frequency of outer electrons in cold uranium, resulting in a more efficient transfer of energy from the α particle to the free electrons. At temperatures higher than a few hundred electron volts, electron thermal velocities are larger than the velocity of the α particle over most of its range. The stopping power decreases because the interaction time is determined by electron motion, rather than by ion motion. In effect, the electrons are moving so fast that slow ions do not have time to transfer energy to the electrons.

As seen in Fig. 3, the range of a 3.5-MeV α particle in uranium at 10 KeV temperature does not scale linearly with density. The range at $10\rho_0$ density is nearly twice as long (42μm) as would be predicted by scaling the 22-mm range at $0.01\rho_0$ density. Physically, the plasma frequency is higher in a denser medium, resulting in a shorter range of impact parameters for which energy is transferred efficiently from the ion to electrons.

Figure 5 shows range versus temperature for a 90-MeV ^{119}Sn ion in uranium. The solid (dashed) curves were calculated using Eqs. (6) and (7), respectively. For all densities, the range is shortened by about a factor of 2 for temperatures around 1 KeV. The physical mechanism for this range shortening is different from that depicted in Fig. 4. The net charge on the ^{119}Sn ion increases with increasing temperature. Thus, the Z^2 factor in Eqs. (2) and (4) is mainly responsible for the range shortening of ^{119}Sn ions. The range of a 90-MeV ^{119}Sn ion in uranium at 10-KeV temperature does not scale linearly with density. The range in uranium at $10\rho_0$ density is nearly twice as long (3.5μm) as would be predicted by scaling the 1.6-mm range in $0.01\rho_0$ density uranium.

V. CONCLUSION

The methods presented in this paper allow computation of energy loss under conditions of high pressure, temperature, and compression in fissile targets. The extreme conditions in such targets can result in dramatic changes in the range of ions compared to that in cold materials. We have described a method for calculating the electronic stopping power of ions of any energy over a large range in density and temperature in targets of high atomic number. We observe that the ranges of 3.5-MeV α particles and 90-MeV ^{119}Sn ions (fission fragments) are shortened only over a limited region of temperatures in uranium. The ranges scale linearly with density only in cold uranium; at high temperatures the ranges in $10\rho_0$ density uranium are up to twice as long as expected by scaling from the range in $0.01\rho_0$ density uranium. It would be of great interest to test the predictions under experimental conditions.

ACKNOWLEDGMENT

This work was supported in part by Contract No. 958301, Jet Propulsion Laboratory, California Institute of Technology, Pasadena, CA 91109.

[1] A. Angelopoulos *et al.*, Phys. Lett. B**205**, 590 (1988).
[2] T.A. Armstrong *et al.*, Z. Phys. A, **331**, 519 (1988).
[3] J.P. Bocquet *et al.*, in *Physics at LEAR with Low-Energy Antiprotons,* edited by C. Amsler *et al.* (Harwood, Switzerland, 1988), p. 793.
[4] S. Polikanov, in *Physics at LEAR with Low-Energy Cooled Antiprotons,* edited by U. Gastaldi and R. Klapisch (Plenum, New York, 1984), p. 851.
[5] J.F. Ziegler, J.P. Biersack, and U. Littmark, *The Stopping and Range of Ions in Solids* (Pergamon, New York, 1985).
[6] J.D. Jackson, *Classical Electrodynamics,* 2nd ed. (Wiley, New York, 1975), p. 641.
[7] N. Bohr, Philos. Mag. **25**, 10 (1913).
[8] U. Fano, Ann. Rev. Nucl. Sci. **13** 1 (1963).
[9] O.B. Firsov, Zh. Eksp. Teor. Fiz. **36**, 1517 (1959) [Sov. Phys. JETP **9**, 1076 (1959)].
[10] K.A. Bruckner, L. Senbetu, and N. Metzler, Phys. Rev. B **25**, 25 (1982).
[11] X. Yan, S. Tanaka, S. Mitake, and S. Ichimaru, Phys. Rev. A **32**, 1785 (1985).
[12] N.A. Tahir and K.A. Long, Phys. Fluids **30**, 1820 (1987).
[13] S. Karashima and T. Watanabe, Laser Part. Beams **5**, 525 (1987).
[14] T.A. Mehlhorn, J. Appl. Phys. **52**, 6522 (1981).
[15] M.N. Saha, Philos. Mag. J. Sci. **40**, 472 (1920).
[16] H. Drawin and P. Felenbok, *Data for Plasmas in Local Thermodynamic Equilibrium* (Gauthier-Villars, Paris, 1965).
[17] V.S. Nikolaev and I.S. Dmitriev, Phys. Lett. **28**A, 277 (1968).
[18] K.A. Long and N.A. Tahir, Phys. Rev. A **35**, 2631 (1987).
[19] E. Nardi and Z. Zinamon, Phys. Rev. Lett. **49**, 1251 (1982).
[20] J.M. Peek, Phys, Rev. A **36**, 5429 (1987).
[21] E.J. McGuire, Phys. Rev. A **26**, 1871 (1982).
[22] D. Menzel *et al.*, *Stellar Interiors* (Chapman and Hall, London, 1963).
[23] S. Knipp and E. Teller, Phys. Rev. **59**, 659 (1941).